

1                   **Analysis of a compounding surge and precipitation event in the**  
2                   **Netherlands**

3  
4                   Bart van den Hurk<sup>1</sup>, Erik van Meijgaard<sup>1</sup>, Paul de Valk<sup>1</sup>, Klaas-Jan van Heeringen<sup>2</sup>  
5                   and Jan Gooijer<sup>3</sup>

6  
7                   <sup>1</sup> KNMI – Royal Netherlands Meteorological Institute, de Bilt, The Netherlands

8   <sup>2</sup> Deltares, Delft, The Netherlands

9   <sup>3</sup> Water board Noorderzijlvest, Groningen, The Netherlands

10  
11  
12                   Submitted to Environmental Research Letters (special issue Knowledge for  
13                   Climate)

14  
15  
16                   Version 7 November 2014

17  
18                   **Abstract**

19                   Hydrological extremes in coastal areas in the Netherlands often result from a  
20                   combination of anomalous (but not necessarily extreme) conditions: storm  
21                   surges preventing the ability to discharge water to the open sea, and local  
22                   precipitation generating excessive water levels in the inland area. A near-flooding  
23                   event in January 2012 occurred due to such a combination of (mild) extreme  
24                   weather conditions, by which free discharge of excessive water was not possible  
25                   for 5 consecutive tidal periods.

26  
27                   An ensemble of regional climate model simulations (covering 800 years of  
28                   simulation data for current climate conditions) is used to demonstrate that the  
29                   combined occurrence of the heavy precipitation and storm surge in this area is  
30                   physically related. Joint probability distributions of the events are generated from  
31                   the model ensemble, and compared to distributions of randomized variables,  
32                   removing the potential correlation. A clear difference is seen. An inland water  
33                   model is linked to the meteorological simulations, to analyse the statistics of  
34                   extreme water levels and its relationship to the driving forces. The role of the  
35                   correlation between storm surge and heavy precipitation increases with inland  
36                   water level up to a certain value, but its role decreases at the higher water levels  
37                   when tidal characteristics become increasingly important.

38  
39                   The case study illustrates the types of analyses needed to assess the impact of  
40                   compounding events, and shows the importance of coupling a realistic impact  
41                   model (expressing the inland water level) for deriving useful statistics from the  
42                   model simulations.

43  
44                   **Keywords**

45                   Compounding events; flooding; coastal water management.

46

## 47 **Introduction**

48 The adaptation to climate conditions by societies across the planet is frequently  
49 challenged by large impacts of weather extremes. However, the magnitude of  
50 the impact is rarely uniquely determined by the value of a univariate  
51 meteorological quantity such as rainfall, wind speed, or temperature. In practice  
52 it is a combination of circumstances that lead to a high impact event, either of  
53 meteorological nature only (heavy rains in combination with a wind driven storm  
54 surge, a long drought in combination with high temperatures) or a mixture of  
55 meteorological conditions and non-meteorological issues (such as high population  
56 density, poor infrastructure). It is of high relevance to consider the contribution  
57 of compounding circumstances and processes when analysing high impact events  
58 and their possible trends.

59

60 In the IPCC Special Report on climate Extremes (SREX, Seneviratne et al., 2012)  
61 compounding events are defined as (among other definitions) "combinations of  
62 events that are not themselves extreme but lead to an extreme event or impact  
63 when combined". Leonard et al. (2014) reviewed the SREX definitions, and  
64 emphasized the necessity of establishing a statistical relationship between the  
65 different events. More generally, in order to be able to make quantitative  
66 assessments of the importance, frequency or trends in compounding events both  
67 a modelling framework and a good definition of temporal and spatial scales is  
68 necessary. Taking the global scale as sampling domain it will be easy to  
69 demonstrate the simultaneous occurrence of two arbitrary events, but the spatial  
70 and temporal characteristics of these events determine the actual impact on  
71 society.

72

73 The analysis of the statistical properties of compounding events requires the  
74 modelling of joint probabilities. Various examples exist in literature (see Leonard  
75 et al. (2014) for an extensive review), making use of statistical tools as copulas  
76 (e.g. Lian et al. 2013), Bayesian networks (Gutierrez et al. 2011), correlation  
77 metrics (Zheng et al. 2013) or physical modelling (Kew et al. 2013; Klerk et al.  
78 2014).

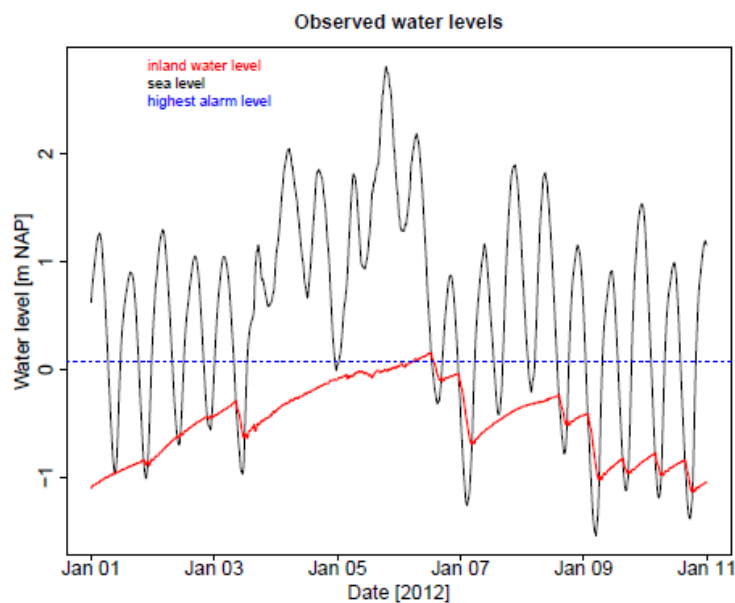
79

80 Diagnosing extreme events from a limited observational record is a challenge,  
81 and can sometimes be bypassed by pooling observations from multiple stations  
82 (Zheng et al. 2013) or using large physical model ensembles (Kew et al. 2013).  
83 Under the constraint that the joint occurrence of relevant processes or metrics is  
84 modelled well, long simulations of "virtual" weather events lead to a solid  
85 estimation of the statistical properties of these joint occurrences. In addition,  
86 coupling to impact assessment modules allows focusing on the events that have  
87 a high impact on the society (Berkhout et al. 2013), and can be used to analyse  
88 non-stationary systems due to for instance climate change or altered land use or  
89 infrastructure arrangements (Hazeleger et al. 2014).

90

91 In this paper we illustrate the application of a regional climate model ensemble  
92 to analyse the compounding occurrence of heavy precipitation and storm surge  
93 conditions in a Dutch coastal polder area. Its water balance is determined by the  
94 difference in local rainfall runoff and the amount of discharge to the sea under  
95 low tide conditions. A near flooding event in January 2012 exposed the  
96 vulnerability of this area to these compounding events. The meteorological  
97 model, coupled to a local water balance model, is used to quantify the effect of  
98 correlation between rainfall and storm surge on inland water levels, for relevant  
99 time scales. Analyses for future climate conditions are to be described in a  
100 follow-up paper.

101



102

103 *Figure 1: Observed water level in the North Sea (black line) and inland water*  
104 *level close to the Lauwersmeer outlet to the North Sea (red line) during the first*  
105 *3 weeks of Januari 2012. Between 4 and 7 Januari five consecutive low tide*  
106 *episodes did not allow any discharge of inland water to the North Sea. The blue*  
107 *dotted line refers to the warning level leading to precautionary measures (+7 cm*  
108 *NAP)*

109

### 110 **Description of the area and the near flooding event in 2012**

111 Water management in The Netherlands is organised in regional water boards,  
112 that are more or less aligned with hydrological units. The water board  
113 Noorderzijlvest (1440 km<sup>2</sup>) is situated in the North of the Netherlands, and the  
114 average altitude is similar to the mean sea level. Via two main outlets the  
115 excessive water is discharged through a combination of pumps and inland  
116 storage reservoirs to the Lauwersmeer, and from there drained off into the  
117 North Sea by gravitation during low tides.

118

119 In January 2012 a series of active low pressure systems passed by over the  
120 North Sea from west to east producing >60 mm rain accumulated over 5 days,  
121 and five consecutive tidal periods in which storm surges did not permit any

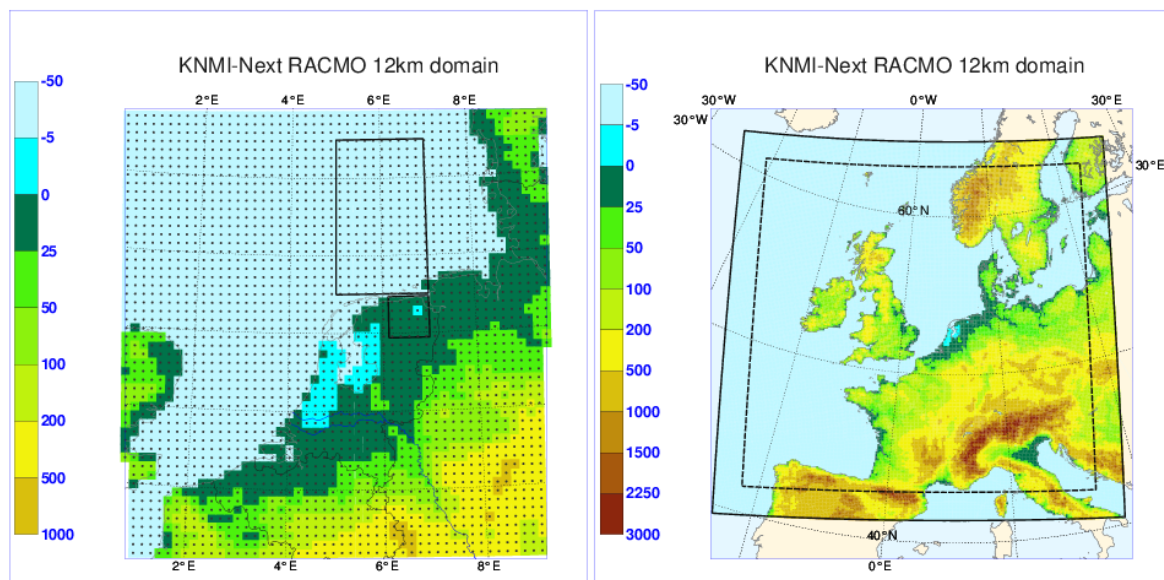
122 gravitational drainage to occur (Figure 1). The soil in the entire area was already  
123 saturated owing to above normal rainfall in the preceding weeks. High inland  
124 water levels (particularly close to the water outlet channel at Lauwersmeer)  
125 exceeding the warning level of +7cm NAP lead to precautionary measures such  
126 as evacuation and the use of emergency overflow areas. The 5-day precipitation  
127 amount had a return time of approximately 10 years, similar to the return time  
128 of the storm surge level. However, an accurate estimate for the return time of  
129 the combined occurrence could not be derived from observations due to the  
130 limited record length.

131

### 132 **Data and Methodology**

133 The get a robust estimate of the return time of the combined events, the  
134 compounding rainfall and storm surge events leading to the situation as  
135 described above have been analysed using an ensemble of Regional Climate  
136 Model (RCM) simulations (operated at high spatial resolution similar to Numerical  
137 Weather Prediction (NWP) applications), driving a hydrological management  
138 simulator generating time series of inland and North Sea water levels.  
139 Precipitation output was corrected with a non-linear bias correction scheme, and  
140 storm surge was empirically derived from simulated outbound wind conditions.

141



142

143 *Figure 2: Grid spacing (left) and simulation domain (right) of the RACMO2 RCM.*

144 *Initial and boundary conditions are provided by the EC-Earth climate model.*

145 *Boxes in left panel show areas of analysed precipitation in the target domain*  
146 *(lower box), and wind speed used to generate coastal storm surge (upper box).*

147

### 148 The atmospheric model

149 The RCM used is RACMO2 (Van Meijgaard et al. 2008; Van Meijgaard et al.  
150 2012), forced with information from the global climate model EC-Earth  
151 (Hazeleger et al. 2012). After spinning-up the ocean component of the global  
152 climate model, an ensemble was produced by perturbing the initial atmosphere

153 state of EC-Earth in 1850 and running each member until 2000 assuming historic  
 154 greenhouse gas concentrations. A corresponding RACMO2-ensemble was  
 155 generated by downscaling each of the EC-Earth members for the period 1950-  
 156 2000, giving  $16 \times 50 = 800$  years of weather representing present day climate  
 157 conditions. The RCM uses prescribed sea surface temperatures generated by EC-  
 158 Earth, and dynamically resolves all meteorological processes at 5 minute time  
 159 steps and 12 km resolution in the domain interior as shown in Figure 2.

160

### 161 Precipitation data

162 Hourly precipitation was derived by averaging RACMO2 output from all grid  
 163 points enclosing the Noorderzijlvest area (see Figure 2). A common feature in  
 164 many GCM driven RCM simulations is a systematic bias in precipitation,  
 165 dependent on biases in the driving GCM, the precipitation processes in the RCM,  
 166 and resolved hydrological feedbacks. Hourly precipitation observations between  
 167 1998 and 2012 were obtained from in situ station data at Lauwersoog. Using  
 168 rainfall radar data, an Area Reduction Factor was applied following Overeem et  
 169 al. (2010), to account for the scale-dependence of the relationship between  
 170 rainfall intensity and return time. A non-linear bias correction (van Pelt et al.  
 171 2012) was applied of the form

172

$$\begin{aligned}
 P^* &= \frac{E_o}{E_c} (P - P_c^{90}) + a(P_c^{90})^b & P > P_c^{90} \\
 P^* &= aP^b & P < P_c^{90}
 \end{aligned}
 \tag{1}$$

174

175 where excess  $E_c$  is the mean precipitation of all precipitation events exceeding  
 176 the modelled 90<sup>th</sup> percentile value ( $P_c^{90}$ ),  $E_o$  the same for the observations,  $P^*$  is  
 177 the corrected precipitation amount and  $a$  and  $b$  are empirically derived bias  
 178 correction coefficients inferred from observed and modelled 60- and 90-  
 179 percentile values of precipitation  $P$ . The bias correction is applied to 5-day  
 180 precipitation sums, which avoids problems with biases in frequency of occurrence  
 181 of wet intervals (Leander and Buishand 2007). Moreover, the 5-day interval  
 182 represents the appropriate time scale for the analysis applied here (see below).  
 183 Experiments with 99-percentile values do not lead to very different results (not  
 184 shown). 3-hourly precipitation time series are derived by assigning a similar  
 185 correction to every 3-hour interval in a given 5-day interval of a particular  
 186 intensity. Figure 3 shows results for 5-day and 3-hourly time series.

187

### 188 Wind and storm surge

189 RACMO2 simulations were not coupled to a dynamic wave model, but instead an  
 190 empirical relationship between 3-hourly instantaneous wind speed  $u$  and  
 191 direction  $\varphi$  and storm surge  $S$  was derived using a regression equation of the  
 192 form (van den Brink et al. 2004)

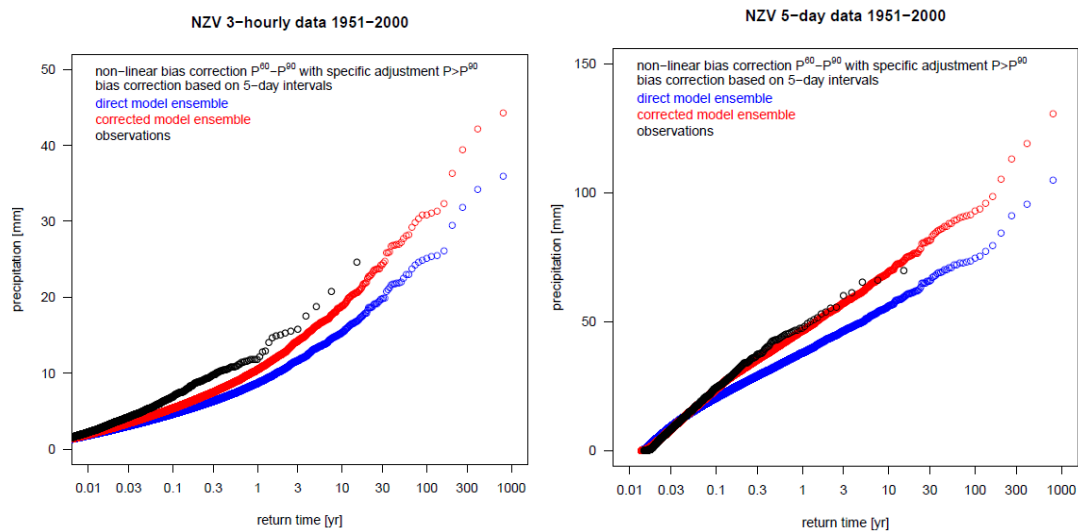
193

$$S = \alpha u^2 \sin(\varphi - \beta)
 \tag{2}$$

194

195

196 where  $\alpha$  and  $\beta$  are regression coefficients. The regression equation was calibrated  
 197 using wind data from RACMO2 model from the North Sea box (see Figure 2) and  
 198 local surge data at station Lauwersoog. Comparison between the observed and  
 199 modelled frequency distribution of the storm surge leads to a good  
 200 correspondence for high surges for 3-hourly averaged values (not shown).  
 201



202  
 203 *Figure 3: Observed, modelled and bias corrected precipitation accumulated over*  
 204 *3-hourly(left) and 5-dai (right) intervals*  
 205

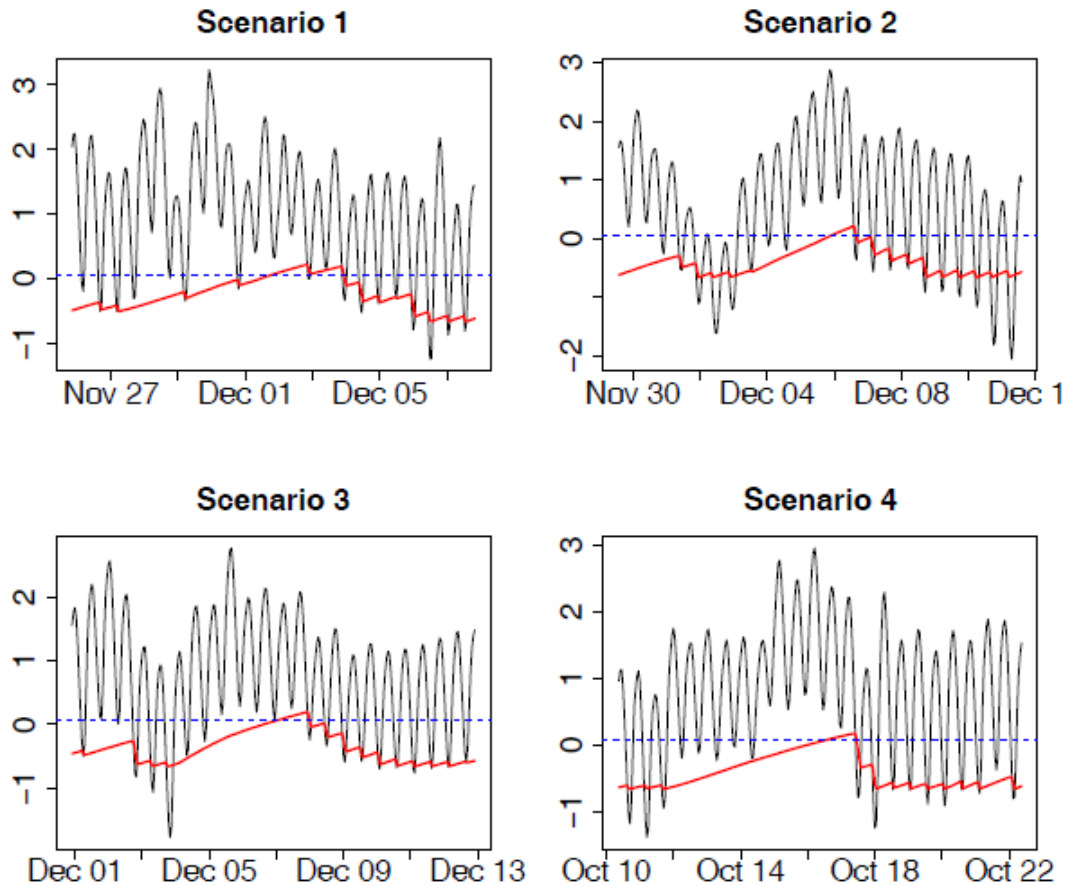
206 The historical astronomical tide between 1950 and 2000 was added to the  
 207 modelled storm surge data, to generate a time series of sea level at the North  
 208 Sea coast. Note that this astronomical tide is not correlated to the meteorological  
 209 phenomena analysed here, and therefore does not affect the statistics of  
 210 compounding events. However, the astronomical tide does play an important role  
 211 in the occurrence of high water levels, as will be discussed below.  
 212

### 213 Simulation of the regional hydrological balance

214 RACMO2 time series of bias corrected hourly precipitation, uncorrected total  
 215 surface evaporation (collected over the same domain as precipitation) and sea  
 216 level were used as a forcing to the so-called RTC-Tools water balance tool. RTC-  
 217 Tools is an open source Real-Time Control modelling tool (see  
 218 <http://oss.deltares.nl/web/rtc-tools/home>). It is used to describe the dynamics  
 219 of the water level in the Noorderzijlvest area, accounting for effects of  
 220 precipitation, evaporation, soil moisture and ground water storage, and  
 221 horizontal transport of water via the managed water system. It consists of a  
 222 number of interacting modules representing subsystems in the water  
 223 management domain, optimized for rapid simulations and data processing, and  
 224 also used in the daily operations of the water board.  
 225

226 RTC-Tools is used to calculate the inland water level at a number of locations in  
 227 the Noorderzijlvest area, including Lauwersmeer (Figure 1). Figure 4 shows  
 228 examples of simulations of the water level at this location, in combination with

229 sea level at Lauwersoog (equivalent to Figure 1). The simulations show  
 230 qualitatively similar events as observed in January 2012, when a multi-day storm  
 231 surge prohibited discharge of high rainfall amounts into the North Sea. A further  
 232 examination of the 800 years of simulation data is discussed in the next section.  
 233



234  
 235 *Figure 4: Snapshots of high water level events simulated by the hydrological*  
 236 *water management model RTC-Tools using RACMOs output as forcing. Shown*  
 237 *are four arbitrary episodes ("scenarios") leading to water levels exceeding the*  
 238 *highest warning level, indicated by the horizontal dotted line.*  
 239

## 240 **Results**

### 241 Compounding precipitation/surge events

242 Figure 5 demonstrates the existence of a correlation between heavy precipitation  
 243 and storm surge. The joint probability distribution resulting from the 800-year  
 244 RCM simulations is compared to the distribution of a set of randomized data in  
 245 which the correlation is removed by combining non-corresponding RCM ensemble  
 246 members. Results are shown for averaging periods of variable length. The  
 247 difference between these joint probability distributions, highlighted in colour in  
 248 the figure, illustrate the physical correlation between the plotted quantities: in  
 249 these areas the probability of finding a combination of a high precipitation and  
 250 high storm surge is larger in the reference runs than in the shuffled simulations.  
 251 We find such enhanced probabilities generally in the upper right (and lower left)

252 corners of the diagram, while the off-diagonal areas show opposite behaviour  
253 (not colour-coded).

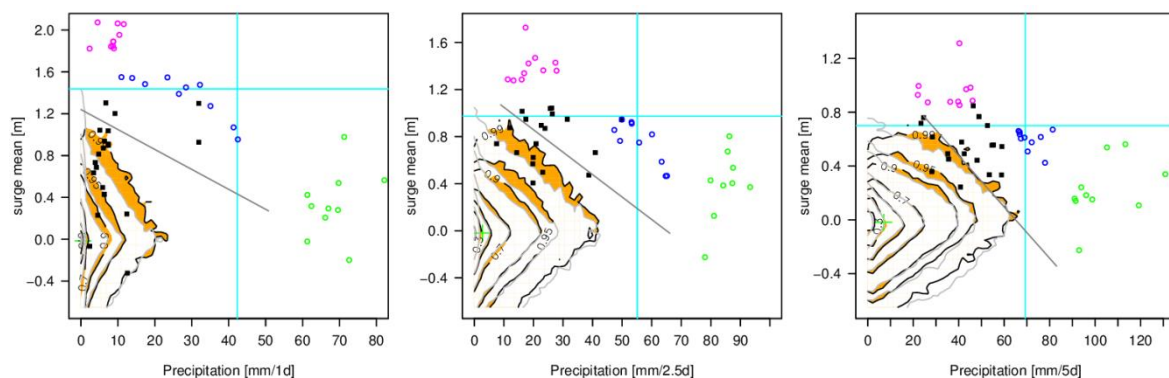
254

255 The existence of a correlation in the high tails of both precipitation and storm  
256 surge points at a common cause: one or multiple active low pressure systems  
257 which set up a strong northerly wind leading to a storm surge, while at the same  
258 time the associated frontal systems produce high amounts of precipitation (see  
259 below for a further exploration of these events).

260

261 In the analyses shown in Figure 5 we have taken the *mean* storm surge in the  
262 indicated time interval. The water balance characteristics of the Noorderzijlvest  
263 area are, however, not governed by the mean sea level within a time interval,  
264 but by the sequence of tidal lows within that period. Examining the relationship  
265 between accumulated precipitation and the single *minimum* sea level in the  
266 accumulation period does not show a clear correlation structure when the  
267 accumulation period is chosen to be 5 days. This single minimum is hardly  
268 related to the average storm characteristics in a 5-day interval, and also does  
269 not affect the local water balance greatly. Therefore, the mean sea level, which is  
270 strongly correlated to the mean level of the tidal lows in that period, is a more  
271 appropriate measure to analyse. For shorter time intervals, containing only one  
272 or two tidal lows, a stronger relationship between mean and single minimum sea  
273 level within that period exists.

274



275

276

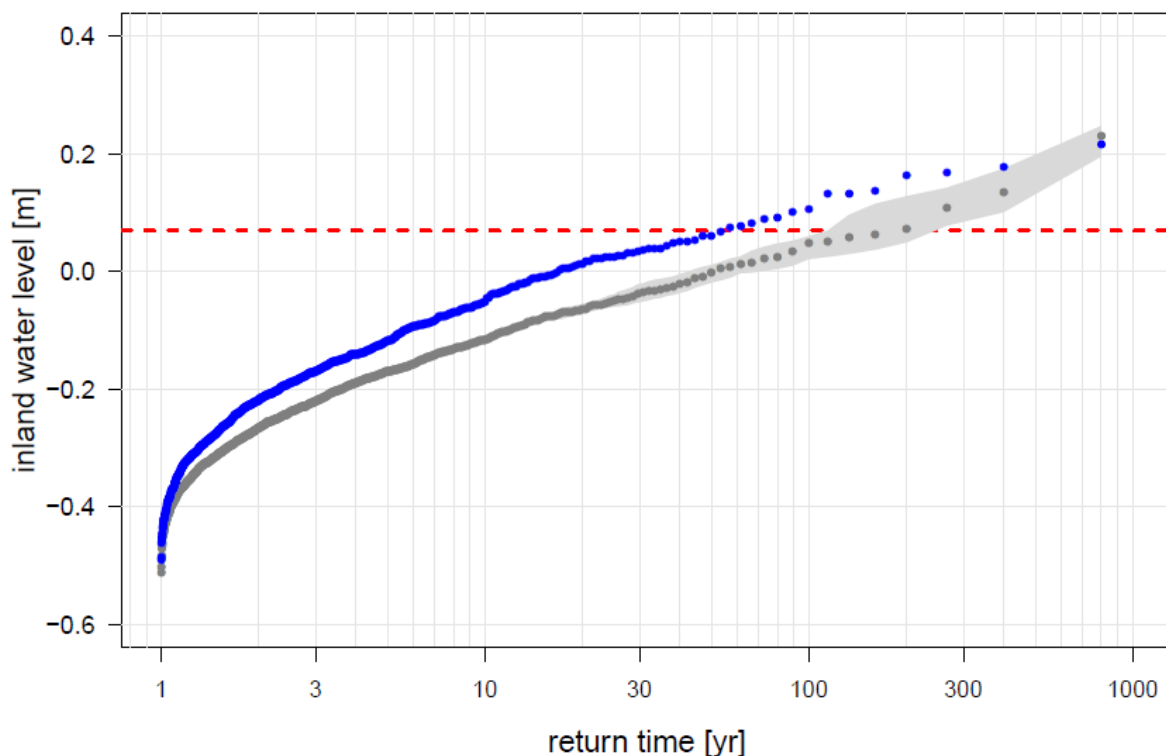
277 *Figure 5: Joint probability distribution of accumulated precipitation in the*  
278 *Noorderzijlvest area and mean surge height for (left) 1, (middle) 2.5 and (right)*  
279 *5 days intervals. Heavy contours denote the area enclosing indicated percentage*  
280 *of data (30, 50, 70, 90, 95 and 99% contours are shown) from the reference*  
281 *RCM simulation, while light contours show these data from the RCM "shuffled"*  
282 *simulations (see text). The orange colored area marks the joint probabilities that*  
283 *are lower for the shuffled data, pointing at physical correlation between the two*  
284 *quantities. The ten events with the most extreme wind-induced surge are*  
285 *plotted in each figure panel (magenta points), similarly for the most extreme*  
286 *precipitation events (green points), and a combination of high wind-induced*  
287 *surge and high precipitation (blue points). The black squares represent the 20*  
288 *events corresponding to the highest inland water level. The vertical and*

289 *horizontal lines (cyan) represent the 10-year return times of precipitation and*  
290 *wind-induced surge for the chosen accumulation period, respectively. The slant*  
291 *grey line, obtained from one and the same prescription in each of the panels, is*  
292 *added for reference.*

293  
294 The different averaging time scales shown in Figure 5 display similar correlation  
295 characteristics: removal of the correlation leads to lower population densities of  
296 events in the upper right sections of the diagram. In neither of the averaging  
297 intervals delays between surge and precipitation are taken into account. Klerk et  
298 al. (2014) point at the importance of discharge delays for much larger  
299 hydrological systems such as the Rhine area. There it takes several days for  
300 excessive rainfall associated to meteorological systems generating strong storm  
301 surges to reach the river outlet at the coast. Kew et al. (2013) show that the role  
302 of this delay is strongly reduced when taking 20-day averaging intervals, and at  
303 this time scale the importance of compounding surge and rainfall extremes is still  
304 relevant. Due to the much smaller areal size of the Noorderzijlvest area and its  
305 immediate proximity to the coast this delay does not play a major role.

306  
307 The bias correction applied to the RCM rainfall data (Eq 1) does affect the shape  
308 of the correlation structure of Figure 5 by repositioning the precipitation data on  
309 the horizontal axes. However, the chronology of the precipitation events (and  
310 thus their correlation with surge events) is unaffected by this bias correction.

311



312  
313 *Figure 6: Return level of inland water level at Lauwersmeer using the original*  
314 *(blue) and shuffled (grey) RACMO2 time series as forcing. In the shuffled*

315 *simulations the simultaneous occurrence of high precipitation and high storm*  
316 *surge is governed randomly, and a bootstrap is applied to the shuffling operation*  
317 *to generate an uncertainty estimate of  $\pm 1$  standard deviation (grey band). The*  
318 *red dashed line indicates the highest warning level for this station.*  
319

#### 320 Effect of compounding extremes on inland water level

321 Calculations with RTC-Tools, yielding 800 years of time series of inland water  
322 levels, were carried out with both the reference RACMO2 simulations and a  
323 bootstrap of 10 different "shuffled" RACMO2 time series, where combinations of  
324 storm surge and precipitation data were taken from arbitrary non-corresponding  
325 RACMO2 ensemble members. This collection of shuffled data sets allows an  
326 uncertainty assessment of the joint occurrence probability.

327

328 The compounding occurrence of heavy precipitation and storm surge has a  
329 distinct impact on the frequency distribution of high inland water levels. Figure 6  
330 displays the return time of the inland water level for both the reference run and  
331 the shuffled simulations. The reference simulation (including the compounding  
332 occurrence) leads to higher inland water levels for all return times exceeding  
333 once per year. The indicated warning level is exceeded on average only 1/150  
334 years in the randomized simulations (without compounding occurrence), while  
335 this warning frequency is more than two times more frequent in the reference  
336 simulations.

337

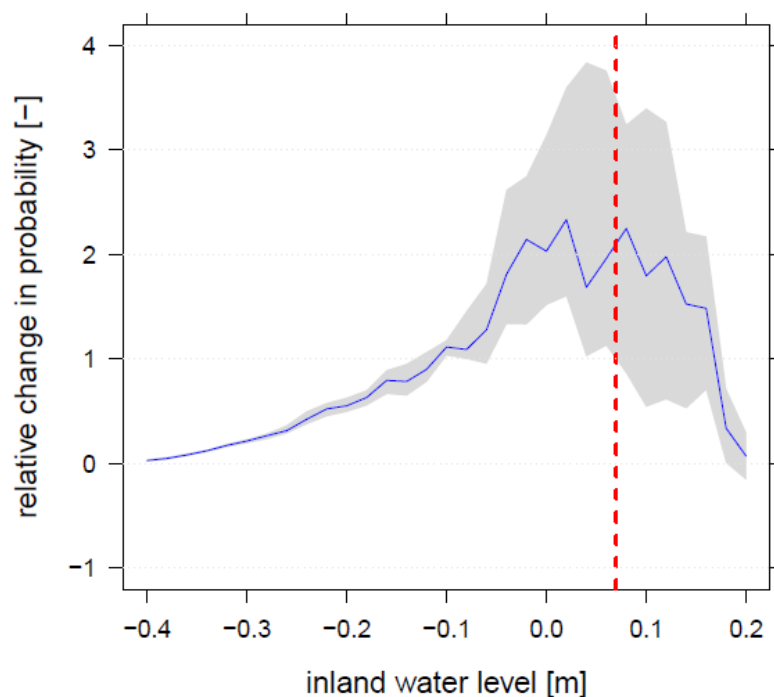
338 The effect of the compounding occurrence is demonstrated in Figure 7, which  
339 shows the relative difference in probability of reaching a given inland water level  
340 derived from the reference simulations and the shuffled simulations, respectively.  
341 This probability ratio is expressed as a function of the inland water level  
342 calculated with RTC-Tools. For inland water levels below the warning level of +7  
343 cm NAP the removal of the compounding occurrence results in a reduction of the  
344 probability of reaching the indicated inland water level by up to a factor 2. The  
345 increase of the relative difference with water level is not just a statistical artefact  
346 created by a reduction of the sample size with increasing water levels: in fact, an  
347 uncertainty estimate generated by a bootstrapping technique does not support  
348 the zero-hypothesis that the relative difference in probability of reaching an  
349 inland water level is independent on the water level. Thus especially for high  
350 water levels – just below the warning level - the effect of compounding events is  
351 of importance. This is supported by the results shown in Figure 5, where, in  
352 particular for high precipitation and storm surge levels (conditions leading also to  
353 high inland water levels), a correlation between these meteorological phenomena  
354 is apparent.

355

356 However, for higher inland water levels the effect of the correlation between  
357 surge and rainfall is reduced, and ultimately disappears for very high water  
358 levels. This is also illustrated in Figure 5, where the precipitation and surge levels  
359 for the events of the 20 highest water levels is indicated (black squares). These

360 events are all positioned in the upper right section of the panels, but not  
361 necessarily in the outer range of the distribution.

362  
363 For these events the astronomical tide appears to play an important role. The  
364 astronomical tide is governed by oscillations in the geometry between Earth,  
365 moon and sun. At spring tide the amplitude between high and low tide is largest,  
366 while at neap tide the amplitude is smallest, implying relatively low levels of high  
367 tide, but also relatively high levels of low tide. Paradoxically, the latter  
368 phenomenon can, dependent on the magnitude of the wind-induced surge,  
369 seriously constrain the amount of gravitational drainage of inland water from the  
370 Lauwersmeer to the North Sea. Closer inspection of the highest inland water  
371 levels reveals that indeed these are usually found under neap tide conditions (not  
372 shown), contributing to discharge limitations under conditions with relatively low  
373 levels of wind-induced surge. Since the astronomical tide is not correlated to the  
374 meteorological conditions, also the effect of removing the correlation between  
375 surge and rainfall is small for the events with the highest inland water levels.  
376



377  
378 *Figure 7: Effect of removing the compound occurrence of high precipitation and*  
379 *storm surge levels on the inland water level at Lauwersmeer. Shown is the*  
380 *relative difference in probability of reaching an inland water level derived from*  
381 *the reference simulations and the shuffled simulations as a function of the inland*  
382 *water level itself. The grey band shows the uncertainty range obtained by*  
383 *bootstrapping the shuffled RACMO2 time series. The red dotted line marks the*  
384 *warning level of +7 cm NAP.*

385  
386 Meteorological situation during extremes

387 Events with extreme 5-day mean wind-induced surge at Lauwersoog primarily  
388 occur during the months October to December. Synoptically they can be  
389 characterized by deep and extensive low pressure systems moving from Iceland  
390 to central or northern Scandinavia with significant anti-cyclonic development  
391 across Ireland and the British Isles in their rear track. This situation gives rise to  
392 strong winds between west and north across the central and northern section of  
393 the North Sea with an associated long wind fetch. Typically, during a 5-day  
394 period one or two of such low pressure systems pass by. Precipitation in the  
395 Noorderzijlvest area is produced by frontal systems, but usually amounts are not  
396 excessive because strong upper air flows in these conditions rapidly push the  
397 frontal systems across the relatively small-scale area. In these situations a  
398 prolonged cyclonic flow of unstable air often extends far south into Central  
399 Europe resulting in huge amounts of orographically induced precipitation on the  
400 lee side of the low-mountain ranges in Belgium and Germany and, in particular,  
401 the high-mountain range of the Alps.

402

403 A summary of the meteorological situation corresponding to extreme wind-  
404 induced surge is shown in Figure 8 (left panel), displaying a composite of  
405 precipitation, surface pressure and wind speed for the ten highest storm surge  
406 events (indicated by magenta symbols in Figure 5).

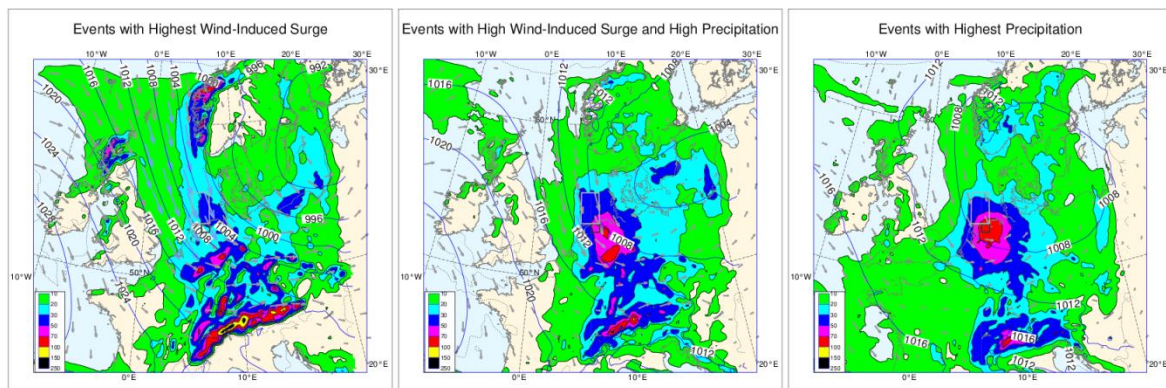
407

408 The right panel in Figure 8 shows the composite of the ten most extreme  
409 simulated precipitation events in the Noorderzijlvest area (green symbols in  
410 Figure 5). The majority of these events occur during the summer months.  
411 Synoptically, a common feature of these events is that a slow-moving medium-  
412 sized low pressure system is positioned close to the area, mostly over Northern  
413 Germany or Southern Denmark, such that associated frontal bands near the  
414 center of low pressure produce considerable amounts of precipitation during  
415 multiple days in the same location. Interestingly, the preferential position of the  
416 center of low pressure gives rise to a north-westerly/northerly flow over the  
417 North Sea, and thus positive wind-induced surge at Lauwersoog. This outcome is  
418 indicative of the feature that for this type of stagnant low pressure systems the  
419 most active bands with precipitation are found in the south-westerly quadrant of  
420 the system, which is where Noorderzijlvest is located relative to Northern  
421 Germany. Eventually, these systems recede, often in easterly direction, or simply  
422 dissipate over time. The onset of this type of synoptic pattern is less  
423 unequivocal, as the low pressure systems giving rise to these high precipitation  
424 events do not follow a preferential track of motion but are found to originate  
425 from a variety of directions.

426

427 Synoptically, the combination of high 5-day mean surge and precipitation  
428 amounts forms a kind of hybrid of the extreme wind-induced surge events and  
429 extreme precipitation events. These events are found year-round, but the  
430 preferential period ranges from end of July to October. The central panel in  
431 Figure 8 shows a composite by selecting events with a surge height exceeding

432 0.8 m (about 10% above the 10-year return time) and 5-day precipitation sum  
 433 above 90 mm (about 20% above the 10-year return time). Compared to the  
 434 extreme wind-induced surge events (left panel in Figure 8) the low pressure  
 435 systems in this sample are smaller in horizontal extent and less deep in central  
 436 pressure. The low pressure systems move predominantly from Scandinavia  
 437 across Eastern Europe in southerly/southeasterly direction, but occasionally  
 438 travel from France over Germany in northeasterly direction. Precipitation during  
 439 these events is primarily produced by frontal bands on the western/south  
 440 western edge of the pressure system and probably enhanced by late summer  
 441 high sea surface temperatures. The low pressure systems and associated frontal  
 442 zones move faster than those associated with extreme precipitation events (right  
 443 panel in Figure 8). Due to the prevalent northerly flow over Germany in this  
 444 synoptic sample the location with maximum precipitation is found over the  
 445 Sauerland low-mountain range.  
 446



447  
 448 *Figure 8: Composite synoptic structure of typical high surge events at*  
 449 *Lauwersoog and/or high precipitation events at Noorderzijlvest obtained from the*  
 450 *full 16 times 50 years of RACMO simulations. Shown are samples of events*  
 451 *corresponding to extreme wind-induced surge (left panel), extreme precipitation*  
 452 *(right panel), and a combination of high wind-induced surge and high*  
 453 *precipitation (central panel). Each sample is composed from the ten most*  
 454 *extreme events, corresponding to those shown in the right-hand panel of Figure*  
 455 *5. Each event is composed as a 5-day mean field for mean sea level pressure*  
 456 *and near surface wind and 5-day accumulated field for precipitation. The black*  
 457 *and grey box indicate the target domains used in determining precipitation and*  
 458 *wind-induced surge, respectively, comparable to Figure 2.*  
 459

## 460 Discussion and conclusions

461 The compounding occurrence of multiple meteorological events leading to critical  
 462 inland water levels in a Dutch coastal polder area is shown to be a factor of  
 463 importance. Safety measures to protect the inhabitants against disruptive  
 464 circumstances are guided by the assessment of the probability of occurrence of  
 465 such events. Insights in the role of correlated phenomena is crucial for this  
 466 assessment.  
 467

468 Here we demonstrate that high surge and high rainfall events tend to be  
469 mutually related by their common dependence on the meteorological situation.  
470 While peak storm surges occur in the winter season as a result of deep cyclones,  
471 high precipitation events are mainly found during stagnant summer depressions.  
472 The meteorological conditions that lead to a combination of these two are  
473 dominantly found around the fall season, and result in a physically based  
474 correlation structure that affects the occurrence of inland high water levels.  
475 Extreme inland water levels are further enhanced during neap tide conditions,  
476 that is uncorrelated to meteorological phenomena.

477  
478 The analysis of climate records supporting the assessment of current or expected  
479 impacts of extreme weather conditions on society should take the notion of  
480 compounding events into account. Typical analyses of climate change driven  
481 trends in weather extremes impacting on society consider univariate  
482 meteorological quantities such as extreme precipitation, wind, or storm surge  
483 (e.g., IPCC 2013). However, this focus on univariate phenomena enhances the  
484 risk of overlooking important combinations of phenomena, or may  
485 overemphasise risks when compounding compensating effects are in place.  
486 Addressing compounding extremes puts the specific local vulnerabilities central  
487 to the analysis of interest (e.g. Brown et al. 2012; Berkhout et al. 2013), and  
488 offers new ways of making relevant assessments of climate driven changes in  
489 risks.

490  
491 The focus on local conditions is central to the analysis of compounding extremes,  
492 as is illustrated in this case study. Time scales, phenomena, spatial scales,  
493 infrastructural operations and non-correlated physical phenomena such as  
494 astronomical tide all play a role. This makes the study of compounding events  
495 and their impacts conceptually challenging: every local situation is unique, and  
496 requires a context specific set-up.

497  
498 The application illustrated here is associated with a number of potential caveats,  
499 that should be taken into account. First, the analysis is heavily based on (long  
500 simulations with) a local water balance model and a regional climate model  
501 driven by forcings from a global climate model, which are all shown to be  
502 imperfect. Inland water level calculations rely on assumptions on the drivers of  
503 the regional water balance in the catchment area. Bias corrections are needed to  
504 adjust the precipitation record, and empirical data are needed to estimate storm  
505 surge data. A systematic bias in the correlation between the occurrences of these  
506 phenomena may likewise be present in the model time series, and may affect the  
507 results significantly. However, due to the lack of long-term reliable observational  
508 records, and to the complex nature of the interaction between atmospheric  
509 circulation, wind driven storm surge, heavy precipitation and soil saturation, the  
510 detection and removal of a bias in this interaction is not straightforward. Further  
511 work in this direction should increase our confidence in the modelling tools  
512 proposed and applied in this paper.

513

514 Second, although an 800-year simulation record was available, the confidence  
515 range of the joint occurrence of events with a return time of 10 years or longer is  
516 still fairly wide. The statistical confidence can be improved by extending the  
517 simulation record length, although it must be recognized that the quality of  
518 model simulations of extreme events with such long return times is difficult to  
519 assess.

520

521 Third, some prior assumptions about the functioning of the local water system  
522 are necessary before analysing the effect of compounding extremes. In our  
523 illustrative case study we explored the effect of different time scales and effects  
524 of astronomical tide, but inevitably have not considered a number of other  
525 important components that may be of relevance. One such component is the  
526 precipitation history that affects the available water storage capacity in the soil  
527 and open reservoirs, which may have played a significant role in the January  
528 2012 event. Other components, not explored here but potentially important, are  
529 the horizontal water transport characteristics in the area, the effect of winds on  
530 open water in the polder area, temperature anomalies affecting evaporation or  
531 convection etc. A formal analysis of all potentially important compounding events  
532 is hardly possible without having (observationally based) evidence on the full  
533 functioning of the system.

534

535 The use of a model set-up as applied here opens the way to analyse effects of  
536 systematic changes in the climatic or infrastructural conditions. Future climate  
537 simulations are available for the RACMO2/EC-Earth configuration, and analysis of  
538 these is subject of ongoing research. However, the credibility of future  
539 assessments depends strongly on the confidence we have in the quality of such  
540 model-based future assessments, which is difficult to support from observational  
541 evidence. For the case study explored here it is evident that assumed changes in  
542 the mean sea level play a strong role in the frequency of high inland water  
543 levels. A good physical understanding of the underlying mechanisms that  
544 potentially lead to a change in the occurrence of compounding events can be  
545 supported by such model analyses.

546

### 547 **Acknowledgements**

548 This study is financially supported by the Dutch Ministry of Infrastructure and  
549 Environment. Discussions with Marc de Rooy, Frank Hallie, the Dutch Delta  
550 Program and colleagues from HKV – Lijn in Water and water board  
551 Noorderzijlvest are highly appreciated.

552

### 553 **References**

554 Berkhout, F., B. Van den Hurk, J. Bessembinder, J. De Boer, B. Bregman, and M.  
555 Van Drunen, 2013: Framing climate uncertainty: socio-economic and  
556 climate scenarios in vulnerability and adaptation assessments. *Reg.*  
557 *Environ. Change*, doi:10.1007/s10113-013-0519-2.

- 558 Van den Brink, H. W., G. P. Können, J. D. Opsteegh, G. J. van Oldenborgh, and  
559 G. Burgers, 2004: Improving 104-year surge level estimates using data of  
560 the ECMWF seasonal prediction system. *Geophys. Res. Lett.*, **31**, L17210,  
561 doi:10.1029/2004GL020610.
- 562 Brown, C., Y. Ghile, M. Laverty, and K. Li, 2012: Decision scaling: Linking  
563 bottom-up vulnerability analysis with climate projections in the water  
564 sector. *Water Resour. Res.*, **48**, W09537, doi:10.1029/2011WR011212.
- 565 Gutierrez, B. T., N. G. Plant, and E. R. Thieler, 2011: A Bayesian network to  
566 predict coastal vulnerability to sea level rise. *J. Geophys. Res. Earth Surf.*,  
567 **116**, F02009, doi:10.1029/2010JF001891.
- 568 Hazeleger, W., and Coauthors, 2012: EC-Earth V2.2: description and validation  
569 of a new seamless earth system prediction model. *Clim. Dyn.*, **39**, 2611–  
570 2629, doi:10.1007/s00382-011-1228-5.
- 571 —, B. J. J. M. Van den Hurk, E. Min, G. J. Van Oldenborgh, A. C. Petersen, D.  
572 A. Stainforth, E. Vasileiadou, and L. A. Smith, 2014: Tales of Future  
573 Weather. *Nat. Clim Change*, **in press**.
- 574 IPCC, 2013: *Climate Change 2013: The Physical Science Basis. Contribution of*  
575 *Working Group I to the Fifth Assessment Report of the Intergovernmental*  
576 *Panel on Climate Change*. Stocker, T. et al., Eds. Cambridge University  
577 Press, Cambridge, United Kingdom and New York, NY, USA.,.
- 578 Kew, S. F., F. M. Selten, G. Lenderink, and W. Hazeleger, 2013: The  
579 simultaneous occurrence of surge and discharge extremes for the Rhine  
580 delta. *Nat. Hazards Earth Syst. Sci.*, **13**, 2017–2029, doi:10.5194/nhess-  
581 13-2017-2013.
- 582 Klerk, W. J., H. C. Winsemius, W. Van Verseveld, A. M. R. Bakker, and F. D.  
583 Diermanse, 2014: The co-occurrence of storm surges and extreme  
584 discharges within the Rhine-Meuse Delta. *Environ. Res. Lett.*, **submitted**.
- 585 Leander, R., and T. A. Buishand, 2007: Resampling of regional climate model  
586 output for the simulation of extreme river flows. *J. Hydrol.*, **332**, 487–496,  
587 doi:10.1016/j.jhydrol.2006.08.006.
- 588 Leonard, M., and Coauthors, 2014: A compound event framework for  
589 understanding extreme impacts. *Wiley Interdiscip. Rev. Clim. Change*, **5**,  
590 113–128, doi:10.1002/wcc.252.
- 591 Lian, J. J., K. Xu, and C. Ma, 2013: Joint impact of rainfall and tidal level on flood  
592 risk in a coastal city with a complex river network: a case study of Fuzhou  
593 City, China. *Hydrol Earth Syst Sci*, **17**, 679–689, doi:10.5194/hess-17-  
594 679-2013.
- 595 Van Meijgaard, E., L. H. Van Ulft, W. J. Van de Berg, F. C. Bosveld, B. J. J. M.  
596 Van den Hurk, G. Lenderink, and A. P. Siebesma, 2008: *The KNMI regional*  
597 *atmospheric climate model RACMO, version 2.1*. KNMI,  
598 [http://www.knmi.nl/publications/fulltexts/tr302\\_racmo2v1.pdf](http://www.knmi.nl/publications/fulltexts/tr302_racmo2v1.pdf).

- 599 ---, ---, G. Lenderink, S. R. De Roode, L. Wipfler, R. Boers, and R.  
600 Timmermans, 2012: Refinement and application of a regional atmospheric  
601 model for climate scenario calculations of Western Europe.
- 602 Overeem, A., T. A. Buishand, I. Holleman, and R. Uijlenhoet, 2010: Extreme  
603 value modeling of areal rainfall from weather radar. *Water Resour. Res.*,  
604 **46**, W09514, doi:10.1029/2009WR008517.
- 605 Van Pelt, S. C., J. J. Beersma, T. A. Buishand, B. J. J. M. van den Hurk, and P.  
606 Kabat, 2012: Future changes in extreme precipitation in the Rhine basin  
607 based on global and regional climate model simulations. *Hydrol. Earth*  
608 *Syst. Sci.*, **16**, 4517–4530, doi:10.5194/hess-16-4517-2012.
- 609 Seneviratne, S., and Coauthors, 2012: Changes in Climate Extremes and their  
610 Impacts on the Natural Physical Environment. *Managing the Risks of*  
611 *Extreme Events and Disasters to Advance Climate Change Adaptation*, C.  
612 Field, V. Barros, T. Stocker, and Q. Dahe, Eds., Cambridge University  
613 Press, 109–230 <http://dx.doi.org/10.1017/cbo9781139177245.006>.
- 614 Zheng, F., S. Westra, and S. A. Sisson, 2013: Quantifying the dependence  
615 between extreme rainfall and storm surge in the coastal zone. *J. Hydrol.*,  
616 **505**, 172–187, doi:10.1016/j.jhydrol.2013.09.054.
- 617